Nonlinear Dyn (2012) 67:2455–2465
DOI 10.1007/s11071-011-0159-3

ORIGINAL PAPER

A novel bounded 4D chaotic system

Jianxiong Zhang · Wansheng Tang

Received: 24 April 2011 / Accepted: 5 July 2011 / Published online: 11 August 2011

Abstract This paper presents a novel bounded four-dimensional (4D) chaotic system which can display hyperchaos, chaos, quasiperiodic and periodic behaviors, and may have a unique equilibrium, three equilibria and five equilibria for the different system parameters. Numerical simulation shows that the chaotic attractors of the new system exhibit very strange shapes which are distinctly different from those of the existing chaotic attractors. In addition, we investigate the ultimate bound and positively invariant set for the new system based on the Lyapunov function method, and obtain a hyperelliptic estimate of it for the system with certain parameters.

Keywords Hyperchaos · Ultimate bound · Positively invariant set · Lyapunov function

1 Introduction

During the past four decades, the study of chaos theory and applications has greatly developed in the fields such as mathematics, physics and engineering applications after the pioneering work of Lorenz [1]. In 1999, Chen and Ueta [2] developed a new chaotic attractor called Chen's attractor, which is topologically more complex than the Lorenz's attractor. In 2002, Lü and Chen [3] reported a new chaotic system named Lü system, which bridges the gap between the Lorenz system and the Chen system. Later, Qi et al. [4] proposed a new chaotic system with five equilibria. Chen et al. [5] reported a novel hyperchaotic system only with one equilibrium. Wang [6, 7] presented a multi-scroll chaotic system generated from a new quadratic autonomous system. A new type of four-wing chaotic attractors in three-dimensional (3D) quadratic autonomous systems was studied in [8]. Recently, Dadras and Momeni [9–11] proposed some interesting multi-scroll chaotic and hyperchaotic systems evolved from novel 3D and four-dimensional (4D) smooth quadratic autonomous systems. Differently from the above chaotic systems generated using quadratic functions, the authors [12, 13] reported some new chaotic systems evolved using hyperbolic functions, and studied the chaos control and chaos synchronization of the systems. Xu and Yu [14] presented some multi-scroll chaotic attractors generated using hyperbolic functions. More recently, a novel chaotic system with infinitely many equilibria was proposed in [15], in which the nonlinear term does not satisfy Lipschitz continuity condition. Up to now, chaos generation has attracted the sustained attention of researchers. It is noted that the existing chaotic attrac-

Supported by the National Natural Science Foundation of China No. 61004015, the Research Fund for the Doctoral Program of Higher Education of China No. 20090032120034, and the Program for Changjiang Scholars and Innovative Research Team in University of China.

J. Zhang (✉) · W. Tang
Institute of Systems Engineering, Tianjin University, Tianjin 300072, China
e-mail: jxzhang@tju.edu.cn

tors as those reported above display two types of basic shapes, i.e. the scroll shape or the wing shape.

The estimate of the bound for a chaotic system is of great importance for chaos control and synchronization, which is also a technically difficult task. The concepts of ultimate bound and attractive set of a system serve as important tools for the analysis of the qualitative behavior of a chaotic system [16]. If it is proved that a system has a globally attractive set, then it is shown that the system cannot have equilibria, periodic solutions, quasiperiodic solutions, or chaotic attractors outside the globally attractive set [17]. This will greatly simplify the dynamic analysis of the system. By virtue of Lyapunov function method, the ellipsoidal estimates of the ultimate bound and positively invariant set for the Lorenz system were proposed in [18, 19], and a butterfly-shaped localization set for the Lorenz attractor was given in [20]. Based on a similar method, bound of the hyperchaotic Lorenz–Stenflo system was presented in [21]. Yang and Liu [22] designed a hyperchaotic system from a chaotic system with one saddle and two stable node-foci, and analyzed the ultimate boundedness. It is noted that most of the research in this area has focused on the family of Lorenz chaotic systems. In fact, many chaotic systems are shown to not have a globally attractive set such as those presented in [9–15]. For the systems proposed in [5, 6, 8], it is very hard to construct analytically the set by the Lyapunov functions technique even though there may be a globally attractive set shown from numerical simulation. The study of a chaotic system with both global attractivity and rich dynamics is of great theoretical and practical significance.

This paper presents a novel 4D chaotic system with the nonlinear terms in the form of quadratic function. The complicated dynamics are studied by virtue of theoretical analysis and numerical simulation. It is shown that the new system can display hyperchaos, chaos, quasiperiodic and periodic behaviors, and may have a unique equilibrium, three equilibria and five equilibria respectively corresponding to the different parameters. Additionally, the chaotic attractors of the new system have very strange shapes which are distinctly different from those of the traditional chaotic attractors, such as scroll-shaped and wing-shaped attractors. Moreover, the new system with certain parameters has a globally attractive set. Based on the Lyapunov function method, the ultimate bound and positively invariant set of the new system is investigated, and a hyperelliptic estimate of the ultimate bound and positively invariant set for the system is obtained.

The rest of the paper is organized as follows. Section 2 introduces the system model and analyzes the complicated dynamic properties. Section 3 estimates the bound of the new system, and Sect. 4 draws the conclusions.

2 System model and dynamic properties

Consider the nonlinear system of the form

$$\begin{cases} \dot{x}_1 = a_1 x_1 + a_2 x_4 - x_2 x_3, \\ \dot{x}_2 = -a_3 x_1 + a_4 x_2 + b_1 x_1 x_3, \\ \dot{x}_3 = a_5 x_3 + b_2 x_1 x_2 + b_3 x_1 x_4, \\ \dot{x}_4 = a_6 x_2 + a_7 x_4 - b_4 x_1 x_3, \end{cases} \tag{1}$$

where $x_1, x_2, x_3, x_4 \in R$ are the state variables, and $a_i < 0, i = 1, 2, \ldots, 7$, $b_j > 0, j = 1, 2, 3, 4$ are constant parameters of the system.

Note that when $a_2 = a_3 = b_4 = 0$, system (1) would reduce to the form of the chaotic system proposed in [10]. Nevertheless, system (1) will display a completely different dynamics with that of the chaotic system in [10].

With different parameters a_i and b_i, it is shown that system (1) can display hyperchaos, chaos, quasiperiodic and periodic behaviors. Figures 1, 2, 3 show the strange attractors such as hyperchaos and chaos. The quasiperiodic and periodic orbits are shown in Figs. 4–5, respectively. It needs to be mentioned that the phase portraits of system (1) have very strange and complex shapes. The shapes of the chaotic attractors in Figs. 1–3 are distinctly different from those of the traditional chaotic attractors, such as the scroll-shaped and wing-shaped attractors displayed in the existing chaotic systems. The quasiperiodic and periodic orbits in Figs. 4–5 also have complex and interesting shapes which correspond to the long-periodic motion. For example, the period of the smile-face-shaped periodic orbit in Fig. 5(b) is approximately equal to 81 by simulation. Furthermore, it is shown from simulation that the systems in Figs. 1–5 have the property of global attractivity, and the boundedness of the system will be investigated analytically in Sect. 3. As an important method, Poincaré map can reflect folding properties of

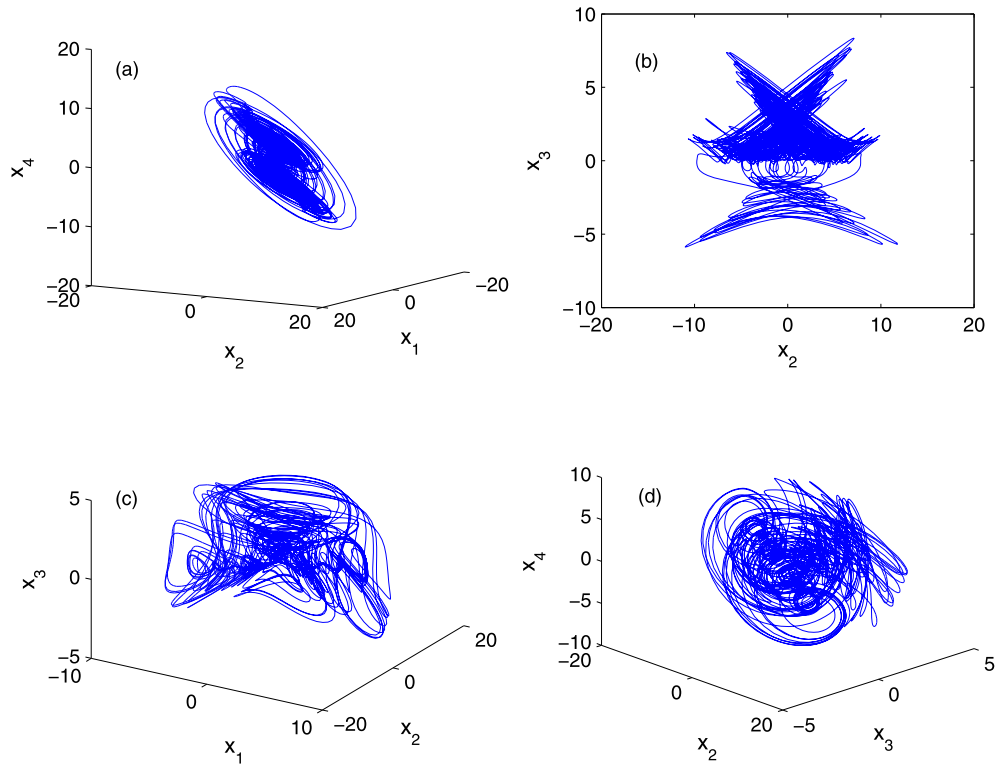

Fig. 1 Phase portraits of system (1) with $a_2 = -0.35$, $a_3 = -0.75$, $a_4 = -0.15$, $a_5 = -0.45$, $a_6 = -0.5$, $a_7 = -0.4$, $b_1 = 1.5$, $b_3 = 1$, $b_4 = 1.15$; (**a**) and (**b**) correspond to the hyperchaotic attractor with $a_1 = -0.16$, $b_2 = 1.1$; (**c**) and (**d**) correspond to the chaotic attractor with $a_1 = -0.4$, $b_2 = 0.55$

chaos. Figure 6 shows the projections of the Poincaré map of system (1) with the parameters in Fig. 3 on different planes.

Additionally, it is obvious that system (1) has the symmetry persisting for all values of the system parameters under the coordinate transform $(x_1, x_2, x_3, x_4) \to (-x_1, -x_2, x_3, -x_4)$, i.e. under reflection about the coordinate axis x_3, and system (1) is not symmetrical about the coordinate axis x_1, x_2 or x_4.

2.1 Equilibria

The equilibria of system (1) can be obtained by solving the following nonlinear algebraic equations simultaneously:

$$\begin{cases} a_1x_1 + a_2x_4 - x_2x_3 = 0, \\ -a_3x_1 + a_4x_2 + b_1x_1x_3 = 0, \\ a_5x_3 + b_2x_1x_2 + b_3x_1x_4 = 0, \\ a_6x_2 + a_7x_4 - b_4x_1x_3 = 0. \end{cases} \tag{2}$$

Obviously the origin $S_0(0, 0, 0, 0)$ is an equilibrium of system (1). For the nonzero equilibria, we have

$$\begin{cases} x_1 = \pm\sqrt{\frac{(k_ia_3 - a_4)a_5a_7}{(a_6b_3 - a_7b_2)b_1 - (k_ia_3 - a_4)b_3b_4}}, \\ x_2 = \frac{1}{k_i}x_1, \\ x_3 = \frac{-a_6b_1b_3 - a_7b_1b_2 - (k_ia_3 - a_4)b_3b_4}{k_ia_5a_7b_1}x_1^2, \\ x_4 = \frac{(k_ia_3 - a_4)b_4 - a_6b_1}{k_ia_7b_1}x_1, \quad i = 1, 2, \end{cases} \tag{3}$$

with

$$k_1 = \frac{B + \sqrt{B^2 - 4a_4a_7A}}{2A},$$

$$k_2 = \frac{B - \sqrt{B^2 - 4a_4a_7A}}{2A},$$

and

$$A = a_1a_7b_1 + a_2a_3b_4, \quad B = a_2a_4b_4 + a_2a_6b_1 + a_3a_7.$$

Therefore, it can be concluded from (3) that in the case of $B^2 < 4a_4a_7A$ system (1) has a unique zero

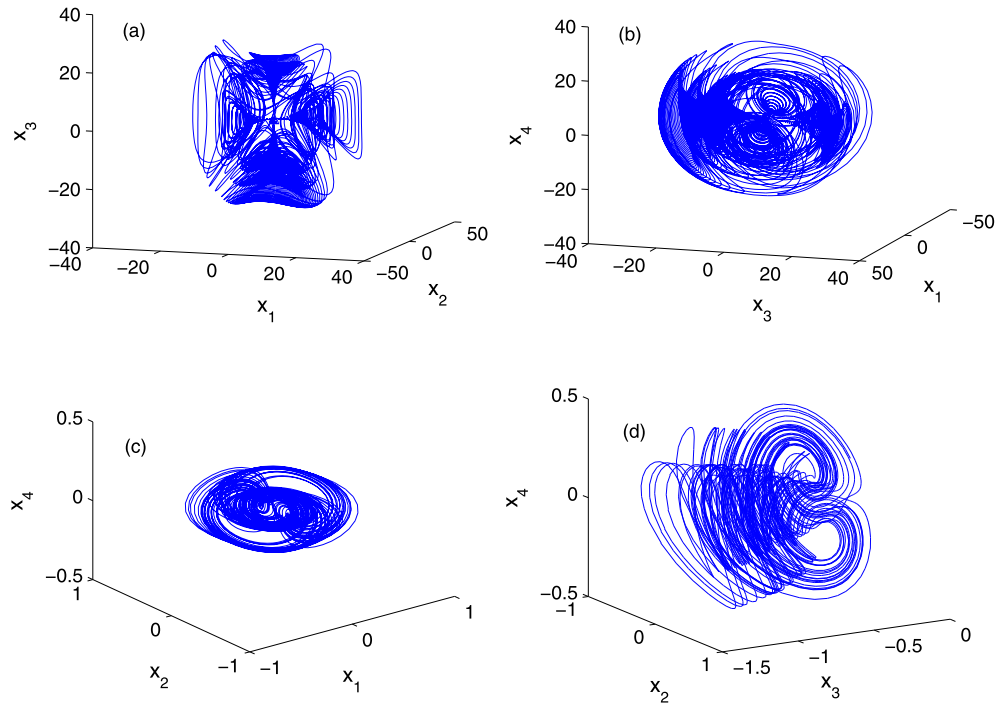

Fig. 2 Chaotic orbits of system (1) with $a_1 = -0.3$, $a_2 = -0.5$, $a_3 = -0.6$, $a_4 = -0.1$, $a_5 = -0.1$, $a_6 = -0.6$, $a_7 = -0.15$, $b_1 = 1.2$, $b_2 = 1.5$, $b_3 = 2.5$; (**a**) and (**b**) correspond to the chaos with $b_4 = 1.9$; (**c**) and (**d**) correspond to the chaos with $b_4 = 0.4$

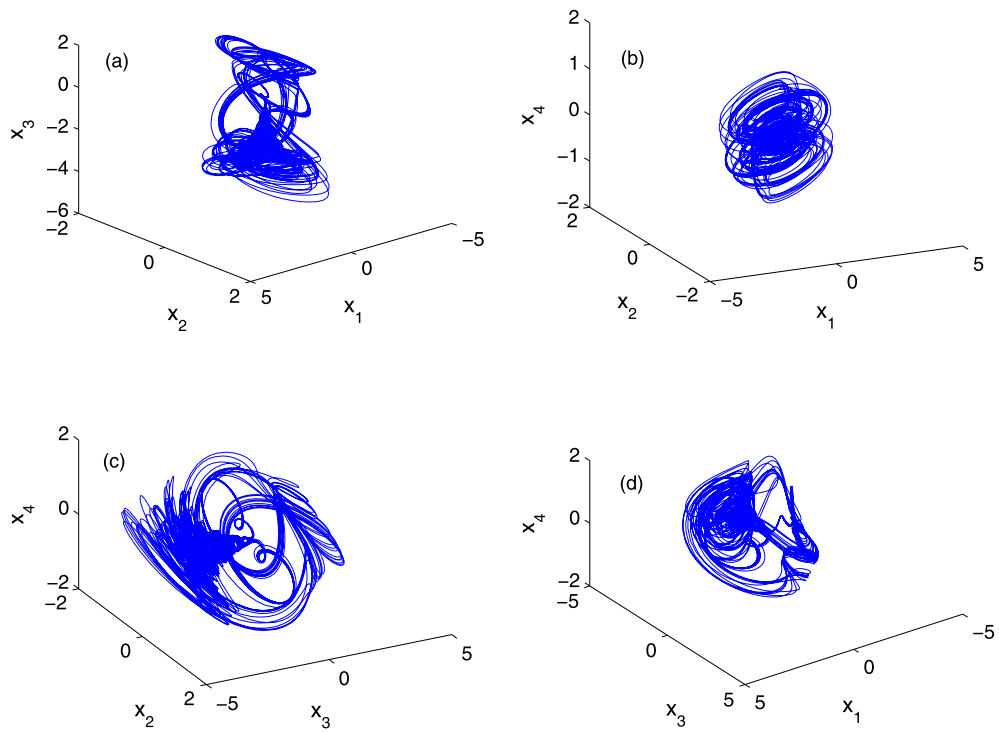

Fig. 3 Chaotic orbits of system (1) with $a_1 = -0.3$, $a_2 = -0.5$, $a_3 = -0.6$, $a_4 = -0.1$, $a_5 = -0.1$, $a_6 = -0.65$, $a_7 = -0.1$, $b_1 = 0.8$, $b_2 = 1.5$, $b_3 = 3$, $b_4 = 0.6$

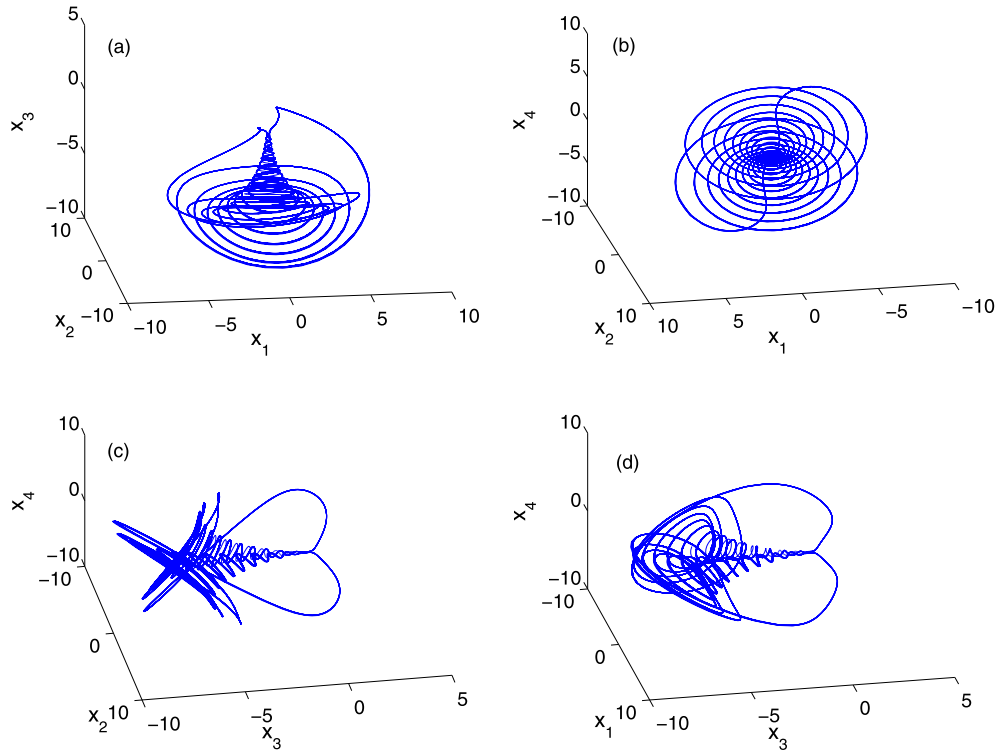

Fig. 4 Quasiperiodic orbits of system (1) with $a_1 = -0.3$, $a_2 = -0.5$, $a_3 = -0.6$, $a_4 = -0.1$, $a_5 = -0.1$, $a_6 = -0.65$, $a_7 = -0.1$, $b_1 = 0.8$, $b_2 = 1.5$, $b_3 = 1$, $b_4 = 0.6$

equilibrium S_0, and in the case of $B^2 = 4a_4a_7A$ system (1) has two nonzero equilibria when inequality (4) holds. In the case of $B^2 > 4a_4a_7A$, system (1) has four nonzero equilibria when inequality (4) holds for both $i = 1, 2$, and system (1) has two nonzero equilibria when the inequality (4) holds only for $i = 1$ or $i = 2$, and system (1) has a unique zero equilibria when inequality (4) holds neither for $i = 1$ nor for $i = 2$.

$$(k_i a_3 - a_4)\big((a_6 b_3 - a_7 b_2)b_1 - (k_i a_3 - a_4)b_3 b_4\big) > 0. \tag{4}$$

It can be verified that for the parameters in Figs. 1, 2(a), 2(b) and 3–5, all with satisfying $B^2 > 4a_4a_7A$, inequality (4) holds neither for $i = 1$ nor for $i = 2$. For the parameters in Figs. 2(c), 2(d) satisfying $B^2 > 4a_4a_7A$, inequality (4) holds only for $i = 1$. Thus, based on the above analysis, the systems which display hyperchaos, chaos, quasiperiodic and periodic behaviors respectively shown in Figs. 1, 2(a), 2(b) and 3–5, all have a unique equilibrium zero, and the system corresponding to the chaos shown in Figs. 2(c), 2(d) has three equilibria.

By linearizing system (1) at the equilibrium S, one obtains the Jacobian matrix as follows:

$$J_s = \begin{bmatrix} a_1 & -x_3 & -x_2 & a_2 \\ -a_3 + b_1 x_3 & a_4 & b_1 x_1 & 0 \\ b_2 x_2 + b_3 x_4 & b_2 x_1 & a_5 & b_3 x_1 \\ -b_4 x_3 & a_6 & -b_4 x_1 & a_7 \end{bmatrix}. \tag{5}$$

For the zero equilibrium S_0, four eigenvalues of the Jacobian matrix J_{s_0} can be obtained from $|\lambda I - J_{s_0}| = 0$, that is

$$(\lambda - a_5)\big(\lambda^3 - (a_1 + a_4 + a_7)\lambda^2 + (a_1a_4 + a_1a_7 + a_4a_7)\lambda + a_2a_3a_6 - a_1a_4a_7\big) = 0. \tag{6}$$

Obviously $\lambda = a_5$ is one negative eigenvalue. It can be seen from (6) that there exists a positive eigenvalue $\lambda > 0$ when $a_2a_3a_6 < a_1a_4a_7$, which is all satisfied for the parameters of the systems displayed in Figs. 1–5, and in this case the zero equilibrium S_0 is unstable. For

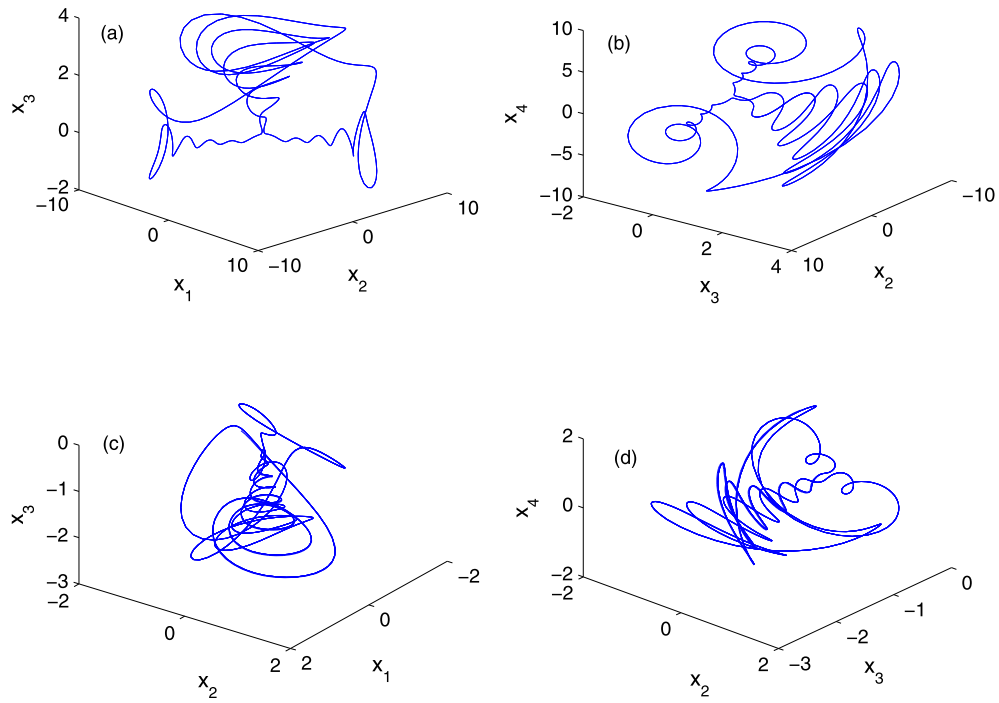

Fig. 5 Periodic orbits of system (1): (**a**) and (**b**) correspond to the system with $a_1 = -0.4$, $a_2 = -0.35$, $a_3 = -0.75$, $a_4 = -0.15$, $a_5 = -0.45$, $a_6 = -0.5$, $a_7 = -0.4$, $b_1 = 1.5$, $b_2 = 0.5$, $b_3 = 1$, $b_4 = 1.15$; (**c**) and (**d**) correspond to the system with $a_1 = -0.3$, $a_2 = -0.5$, $a_3 = -0.6$, $a_4 = -0.1$, $a_5 = -0.1$, $a_6 = -0.6$, $a_7 = -0.15$, $b_1 = 1.2$, $b_2 = 1.5$, $b_3 = 2.5$, $b_4 = 0.8$

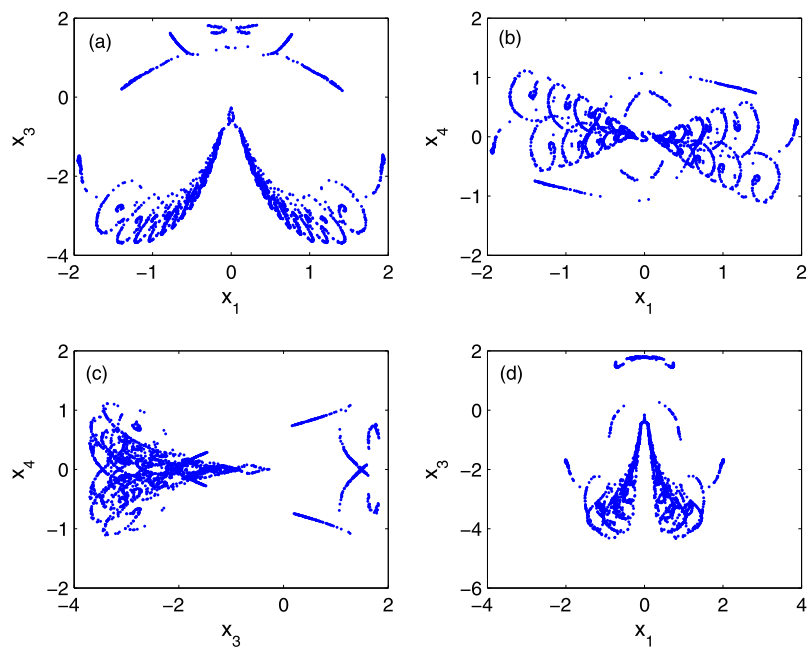

Fig. 6 Poincaré map of system (1) with the parameters in Fig. 3: (**a**)–(**c**) correspond to the cross section with $x_2 = 0$; (**d**) corresponds to the cross section with $x_4 = 0$

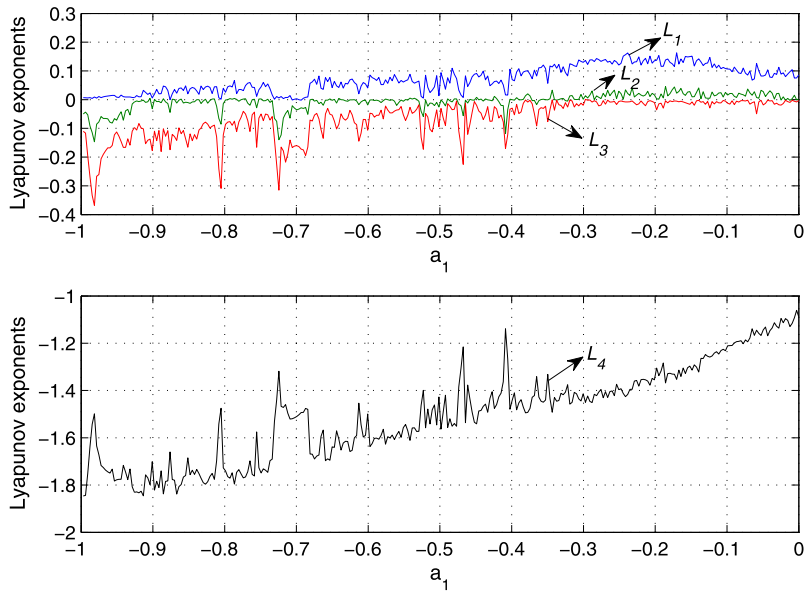

Fig. 7 Spectrum of Lyapunov exponents versus a_1

instance, the eigenvalues of the Jacobian matrix J_{s_0} with the parameters of the hyperchaotic system shown in Fig. 1(a) and (b) can be calculated as

$$\lambda_1 = 0.2833, \quad \lambda_2 = -0.4967 + j0.4275,$$

$$\lambda_3 = -0.4967 - j0.4275, \quad \lambda_4 = -0.45,$$

which implies that the zero equilibrium S_0 is unstable.

Similarly, it can be verified that the nonzero equilibria of the systems with the parameters in Figs. 1–5 are also unstable by computing the eigenvalues from $|\lambda I - J_s| = 0$.

2.2 Dissipativity

From system (1), we obtain

$$\nabla V = \frac{\partial \dot{x}_1}{\partial x_1} + \frac{\partial \dot{x}_2}{\partial x_2} + \frac{\partial \dot{x}_3}{\partial x_3} + \frac{\partial \dot{x}_4}{\partial x_4} = a_1 + a_4 + a_5 + a_7.$$

Thus the dynamical system (1) is a dissipative system when $a_i < 0$, and an exponential contraction of the system is $\exp((a_1 + a_4 + a_5 + a_7)t)$, which implies that each volume containing the trajectory of system converges to a subset of measure zero volume as $t \to \infty$ at exponential rate $-(a_1 + a_4 + a_5 + a_7)$. Then all the orbits of system (1) are eventually confined onto an attractor.

2.3 Lyapunov exponents and bifurcation diagram

Consider the parameters $a_2 = -0.35$, $a_3 = -0.75$, $a_4 = -0.15$, $a_5 = -0.45$, $a_6 = -0.5$, $a_7 = -0.4$, $b_1 = 1.5$, $b_2 = 1.1$, $b_3 = 1$, $b_4 = 1.15$. Figure 7 shows the spectrum of Lyapunov exponents of system (1) with respect to parameters $a_1 \in [-1,\ 0]$. Obviously, when $a_1 \in (-0.4,\ 0]$, the largest Lyapunov exponent is positive, and the second largest Lyapunov exponent is sometimes positive and sometimes equal to zero, which implies that the system displays the hyperchaos and chaos alternately with different values of parameter a_1. When $a_1 \in [-1,\ -0.4]$, the largest Lyapunov exponent is sometimes positive and sometimes equal to zero, and the system displays the chaos, quasiperiodic orbit and periodic orbit alternately with different values of parameter a_1. Particularly, the system is chaotic while the largest Lyapunov exponent is positive and the second largest Lyapunov exponent is zero, and the system displays quasiperiodic motion while the first and the second largest Lyapunov exponents are zero, and displays periodic motion with only one zero Lyapunov exponent. In addition, given $a_1 = -0.16$, we can obtain the Lyapunov exponents as 0.1146, 0.0341, 0 and -1.3084, respectively, which demonstrates that the system shown in Fig. 1(a), (b) is hyperchaotic.

Denote $\Sigma = \{(x_1, x_2, x_3, x_4)^T \in R^4 | x_3 = 0\}$. Taking Σ as a cross section, we can get the bifurcation diagram of state variable x_1 in system (1) with parame-

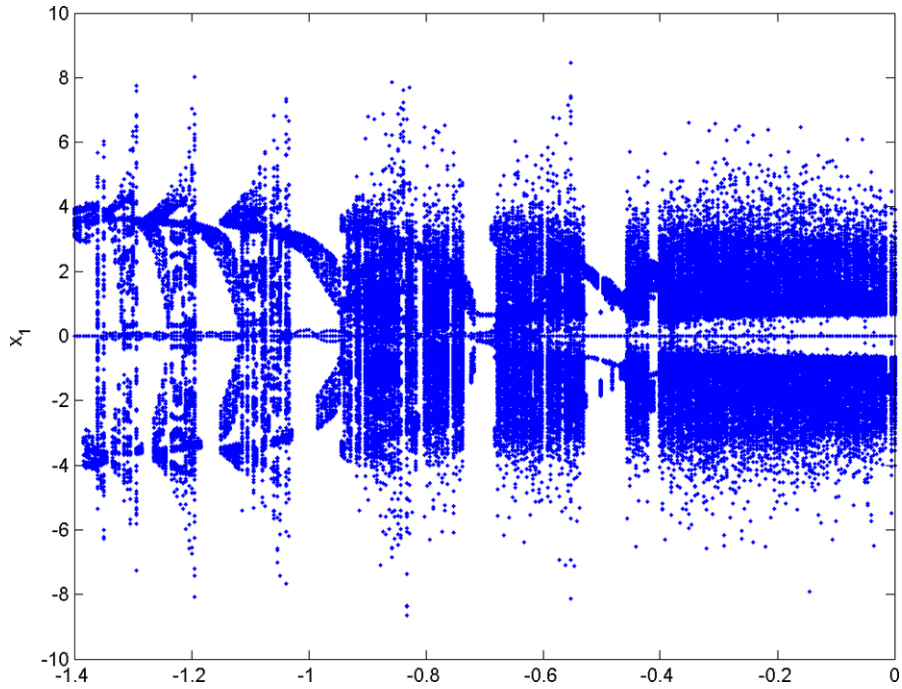

Fig. 8 Bifurcation diagram of x_1 versus a_1

ter $a_1 \in [-1.4,\ 0]$ shown in Fig. 8 which demonstrates the whole dynamic properties versus parameter a_1. It is observed that the bifurcation diagram well coincides with the spectrum of Lyapunov exponents.

3 The ultimate bound and positively invariant set

Let $X = [x_1,\ x_2,\ x_3,\ x_4]^T$. Define $X(t, t_0, X_0)$ as the solution to system (1) satisfying $X(t_0, t_0, X_0) = X_0$ with the initial time t_0 and initial state X_0, which for simplicity is denoted as $X(t)$. Assume $\Omega \in \mathbb{R}^4$ is a compact set. Define the distance between the solution $X(t)$ and the set Ω by $\rho(X(t), \Omega) = \inf_{Y\in\Omega} \|X(t) - Y\|$, and denote $\Omega_\varepsilon = \{X|\ \rho(X, \Omega) < \varepsilon\}$.

Definition 1 Suppose that there is a compact set $\Omega \in \mathbb{R}^4$. If, for every $X_0 \in \mathbb{R}^4 \setminus \Omega$, $\lim_{t\to\infty} \rho(X(t, t_0, X_0), \Omega) = 0$, that is, for any $\varepsilon > 0$ there is $T > t_0$ such that for $t \geq T$, $X(t, t_0, X_0) \in \Omega_\varepsilon$, then the set Ω is called an ultimate bound for system (1). If, for any $X_0 \in \Omega$ and all $t \geq t_0$, $X(t, t_0, X_0) \in \Omega$, then Ω is called the positively invariant set for system (1).

Theorem 1 *If the system parameters satisfy the following inequality*:

$$a_2 b_1 b_2 + \left(a_3 + 2\sqrt{a_1 a_4 b_1}\right) b_3 > 0, \tag{7}$$

then there exist positive constants $\mu > 0$ *and* $C_{\max} > 0$ *such that the hyperellipsoid*

$$\Omega = \left\{ X \middle| \left(b_1\mu + \frac{b_2 b_4}{b_3}\right) x_1^2 + \mu x_2^2 + \frac{b_4}{b_3}\left(x_3 - \frac{a_2 b_1 b_3 \mu + a_2 b_2 b_4}{b_3 b_4}\right)^2 + x_4^2 \leq C_{\max} \right\} \tag{8}$$

is an ultimate bound and positively invariant set for system (1).

Proof With the positive number μ, construct the following Lyapunov function:

$$V(X) = \left(b_1\mu + \frac{b_2 b_4}{b_3}\right) x_1^2 + \mu x_2^2 + \frac{b_4}{b_3}\left(x_3 - \frac{a_2 b_1 b_3 \mu + a_2 b_2 b_4}{b_3 b_4}\right)^2 + x_4^2. \tag{9}$$

The time derivative of the Lyapunov function (9) along the solution of system (1) can be described as

$$\frac{1}{2}\dot{V}(X) = \left(b_1\mu + \frac{b_2 b_4}{b_3}\right) x_1 \dot{x}_1 + \mu x_2 \dot{x}_2$$

$$
\begin{aligned}
&+\frac{b_4}{b_3}\left(x_3-\frac{a_2b_1b_3\mu+a_2b_2b_4}{b_3b_4}\right)\dot{x}_3+x_4\dot{x}_4\\
&=\left(a_1b_1\mu+\frac{a_1b_2b_4}{b_3}\right)x_1^2\\
&\quad+a_4\mu x_2^2+\frac{a_5b_4}{b_3}x_3^2+a_7x_4^2\\
&\quad-\left(a_3\mu+\frac{a_2b_2(b_1b_3\mu+b_2b_4)}{b_3^2}\right)x_1x_2\\
&\quad+a_6x_2x_4-\frac{a_2a_5(b_1b_3\mu+b_2b_4)}{b_3^2}x_3
\end{aligned}
$$

$$
= \tilde{X}^T Q \tilde{X} - C_\mu, \tag{10}
$$

where

$$
\tilde{X} = \left[x_1,\, x_2,\, x_3-\tfrac{a_2b_1b_3\mu+a_2b_2b_4}{2b_3b_4},\, x_4\right]^T,
$$

$$
C_\mu = \frac{a_5(a_2b_1b_3\mu+a_2b_2b_4)^2}{4b_3^3b_4},
$$

and

$$
Q=\begin{bmatrix}
a_1b_1\mu+\frac{a_1b_2b_4}{b_3} & -\frac{a_3\mu}{2}-\frac{a_2b_2(b_1b_3\mu+b_2b_4)}{2b_3^2} & 0 & 0\\
-\frac{a_3\mu}{2}-\frac{a_2b_2(b_1b_3\mu+b_2b_4)}{2b_3^2} & a_4\mu & 0 & \frac{a_6}{2}\\
0 & 0 & \frac{a_5b_4}{b_3} & 0\\
0 & \frac{a_6}{2} & 0 & a_7
\end{bmatrix}.
$$

By some algebra operations, it can be shown that the condition that Q is negative definite is equivalent to

$$
l_1\mu^2+l_2\mu+l_3<0 \tag{11}
$$

with

$$
\begin{aligned}
l_1&=4a_1a_4a_7b_1b_3^4-a_7\left(a_3b_3^2+a_2b_1b_2b_3\right)^2,\\
l_2&=4a_1a_4a_7b_2b_3^3b_4-a_1a_6^2b_1b_3^4\\
&\quad-2a_2a_7b_2^2b_4\left(a_3b_3^2+a_2b_1b_2b_3\right),\\
l_3&=-a_1a_6^2b_2b_3^3b_4-a_2^2a_7b_2^4b_4^2.
\end{aligned}
$$

It can be verified that inequality (7) implies $l_1<0$. Note that $l_3>0$ and $\mu>0$. Then it is easy to show that inequality (11) is equivalent to

$$
\mu>-\frac{1}{2l_1}\left(l_2+\sqrt{l_2^2-4l_1l_3}\right). \tag{12}
$$

Thus for any μ satisfying (12), the matrix Q is negative definite.

Let $\dot{V}(X)=0$. Then one can obtain a 4D hyperelliptic surface as

$$
\Gamma=\left\{X\middle|\tilde{X}^TQ\tilde{X}=C_\mu\right\}. \tag{13}
$$

Note that $V(X)$ is continuous on Γ which is a closed set. It is concluded that the extreme values of $V(X)$ can be achieved on Γ. Denote the maximum value of $V(X)$ as $C_{\max}$, that is, $C_{\max}=\max_{X\in\Gamma}V(X)$. Then, for the 4D hyperellipsoid Ω defined in (8), it is shown that $\Gamma\subset\Omega$.

For any given state variable X outside Ω, which means $\tilde{X}^TQ\tilde{X}<C_\mu$, it is shown that $\dot{V}(X)<0$. In this case, the isoplethic surface of $V(X)$ contracts monotonically along the trajectory of system (1) until $V(X)=C_{\max}$, that is,

$$
\lim_{t\to\infty}\rho\left(X(t),\Omega\right)=0.
$$

Thus Ω is an ultimate bound of system (1).

Furthermore, suppose the maximum value of $V(X)$ on surface Γ is achieved at the point $X^*=(x_1^*,x_2^*,x_3^*,x_4^*)$. For any point $X(t)$ on Ω and $X(t)\neq X^*$, it is derived that $\dot{V}(X)<0$ by the fact $\Gamma\subset\Omega$. Thus any trajectory $X(t)\neq X^*$ of system (1) will go into Ω. In addition, for the case of $X(t)=X^*$, it can be shown that $X(t)$ will also go into Ω by the continuation theorem [23]. Thus Ω is a positively invariant set of system (1).

Summarizing the above, one can conclude that Ω is an ultimate bound and positively invariant set for system (1). The proof is complete. □

For instance, consider the parameters $a_1=a_2=-1.5, a_3=-1.2, a_4=-0.8, a_5=-0.5, a_6=-2, a_7=$

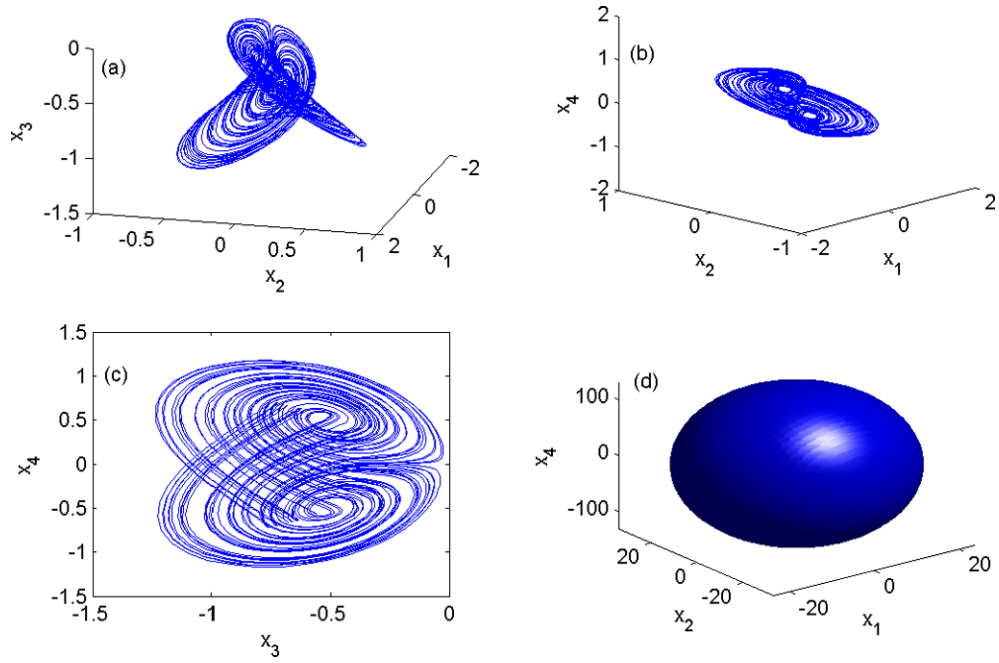

Fig. 9 The chaotic system (1) and its ultimate bound and positively invariant set

-0.3, $b_1 = 2, b_2 = 0.3, b_3 = 1, b_4 = 0.2$, which satisfy inequality (7). It is shown that system (1) displays chaotic orbits. Set $\mu = 15$ with satisfying (12). By solving the corresponding optimization problem, one can obtain that $C_{\max} = \max_{X \in \Gamma} V(X) = 17128$. Thus, according to Theorem 1, the chaotic system (1) with above parameters is confined to the following hyperellipsoid:

$$\Omega = \{X | 30.06x_1^2 + 15x_2^2 + 0.2(x_3 + 225.45)^2 + x_4^2 \leq 17128\}.$$

Figure 9(a)–(c) shows the chaotic orbits, and Fig. 9(d) shows the corresponding ultimate bound and positively invariant set Ω with $x_3 = -225.45$.

4 Conclusion

This paper has introduced a novel 4D chaotic system, which has a unique equilibrium, three equilibria and five equilibria for the different parameters, and shows hyperchaos, chaos, quasiperiodic and periodic orbits with strange shapes. The complex dynamic properties are investigated by means of theoretical analysis and numerical simulation. Moreover, based on the Lyapunov function method, a hyperelliptic estimate of the ultimate bound and positively invariant set for the new system with certain parameters is obtained.

References

1. Lorenz, E.N.: Deterministic nonperiodic flow. J. Atmos. Sci. **20**, 130–141 (1963)
2. Chen, G., Ueta, T.: Yet another chaotic attractor. Int. J. Bifurc. Chaos **9**, 1465–1466 (1999)
3. Lü, J., Chen, G.: A new chaotic attractor coined. Int. J. Bifurc. Chaos **12**, 659–661 (2002)
4. Qi, G., Chen, G., Du, S., Chen, Z., Yuan, Z.: Analysis of a new chaotic system. Physica A **352**, 295–308 (2005)
5. Chen, Z., Yang, Y., Qi, G., Yuan, Z.: A novel hyperchaos system only with one equilibrium. Phys. Lett. A **360**, 696–701 (2007)
6. Wang, L.: 3-scroll and 4-scroll chaotic attractors generated from a new 3-D quadratic autonomous system. Nonlinear Dyn. **56**, 453–462 (2009)
7. Wang, L.: Yet another 3D quadratic autonomous system generating three-wing and four-wing chaotic attractors. Chaos **19**, 013107 (2009)
8. Wang, Z., Qi, G., Sun, Y., van Wyk, M.A., van Wyk, B.J.: A new type of four-wing chaotic attractors in 3-D quadratic autonomous systems. Nonlinear Dyn. **60**, 443–457 (2010)
9. Dadras, S., Momeni, H., Qi, G.: Analysis of a new 3D smooth autonomous system with different wing chaotic attractors and transient chaos. Nonlinear Dyn. **62**, 391–405 (2010)

10. Dadras, S., Momeni, H.: Four-scroll hyperchaos and four-scroll chaos evolved from a novel 4D nonlinear smooth autonomous system. Phys. Lett. A **374**, 1368–1373 (2010)
11. Dadras, S., Momeni, H.: Generating one-, two-, three- and four-scroll attractors from a novel four-dimensional smooth autonomous chaotic system. Chin. Phys. B **19**, 060506 (2010)
12. Zhang, J., Tang, W.: Analysis and control for a new chaotic system via piecewise linear feedback. Chaos Solitons Fractals **42**, 2181–2190 (2009)
13. Zhang, J., Tang, W.: Control and synchronization for a class of new chaotic systems via linear feedback. Nonlinear Dyn. **58**, 675–686 (2009)
14. Xu, F., Yu, P.: Chaos control and chaos synchronization for multi-scroll chaotic attractors generated using hyperbolic functions. J. Math. Anal. Appl. **362**, 252–274 (2010)
15. Zhang, J., Tang, W.: A chaotic system with Hölder continuity. Nonlinear Dyn. **62**, 761–768 (2010)
16. Leonov, G.: Bound for attractors and the existence of homoclinic orbit in the Lorenz system. J. Appl. Math. Mech. **65**, 19–32 (2001)
17. Shu, Y., Xu, H., Zhao, Y.: Estimating the ultimate bound and positively invariant set for a new chaotic system and its application in chaos synchronization. Chaos Solitons Fractals **42**, 2852–2857 (2009)
18. Liao, X.: On the global basin of attraction and positively invariant set for the Lorenz chaotic system and its application in chaos control and synchronization. Sci. China Ser. E **34**, 1404–1419 (2004)
19. Li, D., Lu, J., Wu, X., Chen, G.: Estimating the ultimate bound and positively invariant set for the Lorenz system and a unified chaotic system. J. Math. Anal. Appl. **323**, 844–853 (2006)
20. Suzuki, M., Sakamoto, N., Yasukochi, T.: A butterfly-shaped localization set for the Lorenz attractor. Phys. Lett. A **372**, 2614–2617 (2008)
21. Wang, P., Li, D., Hu, Q.: Bounds of the hyper-chaotic Lorenz–Stenflo system. Commun. Nonlinear Sci. Numer. Simul. **15**, 2514–2520 (2010)
22. Yang, Q., Liu, Y.: A hyperchaotic system from a chaotic system with one saddle and two stable node-foci. J. Math. Anal. Appl. **360**, 293–306 (2009)
23. Lefchetz, S.: Differential Equations: Geometric Theory. Interscience, New York (1963)